Journal of Thermal Analysis and Calorimetry, Vol. 80 (2005) 565–571

APPLICATION OF THERMOMAGNETOMETRY TO CORROSION STUDIES OF ARCHAEOLOGICAL IRON

D. Thickett and M. Odlyha*

School of Biological and Chemical Sciences, Birkbeck College, University of London, London, England

Thermomagnetometry has been applied to mineralised archaeological iron samples and samples from accelerated corrosion tests. It has successfully quantified the degree of corrosion, measured by the loss of iron, as well as the amount of magnetite formed and water held in the corrosion and adhered soil layers. Thermomagnetometry, thermogravimetric analysis and differential scanning calorimetry have been applied to the reported corrosion products from archaeological iron. Fourier transform infra-red and Raman spectroscopies and X-ray diffraction analyses were undertaken on the residues and at intermediate heating stages, where the thermal analyses indicated, to identify the reaction products.

Keywords: *corrosion, DSC, iron, thermomagnetometry, TG*

Introduction

In corrosion studies the quantification of elemental iron is the most common method of determination for the degree of reaction. The mixed nature of corrosion products invalidates simple mass gain as a measure of this. The residual amount of elemental iron is most frequently determined by stripping the corrosion products from the iron surface and then measuring its mass. The requirement for chemical reagents that will dissolve the iron corrosion products, without removing any elemental iron and not cause further corrosion of the iron on extended drying, has not been fully met, requiring complex and time consuming procedures to obtain accurate data [1]. The reagents presently in use also have significant health hazards. Thermomagnetometry provides an alternative or complimentary method to obtain this information from test pieces produced in corrosion tests.

The presence and amount of iron remaining in the un-corroded core of an archaeological object is thought to be an important parameter in the artefacts post excavation corrosion [2]. This information is usually inferred from radiography, examination of cross-sections or the magnetic properties of the object. Thermomagnetometry has been successfully applied to a number of archaeological objects with different ranges of residual iron content. The amount of residual iron in two important iron age tyres was quantified to elucidate their post excavation corrosion behaviour.

Thermomagnetometry is a technique in which a magnetic characteristic of a substance (and/or its reaction product(s)) is measured as a function of temperature whilst the substance is subjected to a controlled temperature program [3]. It has been applied by several workers in the study of iron and its corrosion products [4, 5].

The technique has been calibrated for pure iron, and mixtures designed to mimic the corrosion of archaeological iron. Thermal reactions can produce highly magnetic phases and the thermal reaction pathways of the common iron corrosion products have been studied to identify potential interferences.

It has been applied to a series of accelerated corrosion tests with iron in various soil conditions and to samples of archaeological iron.

Experimental

Thermomagnetometry

Thermomagnetometry was carried out with a Perkin-Elmer TGA7 with 40 cm^3 min^{-1} of nitrogen flowing over the sample in a platinum crucible, and a calibration magnet precisely positioned below the sample to apply a vertical magnetic field. The temperature program for the calibration experiments was: room temperature to 150°C at 50°C min^{-1}; hold for 2 min, the magnet is positioned during this period; 150 to 700°C at 200°C min^{-1}; 700 to 840°C at 20°C min^{-1}.

The TGA7 was initially calibrated *vs*. discs pressed from pure iron powder (Alfa Aesar 99.98%) using a 5 mm die and 2 tonnes force. The TGA7 was then calibrated with samples of known composition designed to mimic the corrosion from archaeological iron. Discs were pressed of iron and of magnetite, Fe_3O_4 and mixtures of goethite, α-FeOOH and

* Author for correspondence: David.Thickett@english-heritage.org.uk

1388–6150/$20.00

Akadémiai Kiadó, Budapest, Hungary
Springer, Dordrecht, The Netherlands

lepidocrite, γ-FeOOH powders were added to mimic the expected morphology of the corroded iron discs, i.e. a metal core, with a thin magnetite layer overlain with powdery corrosion products [6].

The common iron corrosion products found on iron are listed in Table 1. The magnetic properties of these minerals are also included in Table 1 [7]. The magnetic behaviour is dominated by three materials; iron, magnetite and maghemite, γ-Fe_2O_3. These materials have magnetic susceptibilities at least twenty six times greater than any of the other minerals likely to be present. The thermogravimetric behaviour of the other minerals can interfere with the observation of the magnetic transitions if mass changes occur in the same temperature regions as the magnetic transitions. Also thermal transitions that generate the strongly ferrimagnetic corrosion products magnetite and maghemite below their Néel temperatures, will interfere with the determination of these minerals in the sample.

The expected corrosion products of iron were obtained commercially, where possible. Some of the less common corrosion products were also investigated as the study incorporated archaeological iron, which can be exposed to varied environments. Akaganeite, β-FeOOH was synthesised by oxidation of ferric chloride [8]. 500 mL of 0.3 M $FeCl_3$, was heated at 70°C in a sealed glass flask for 48 h. The precipitate was collected by centifuging, washed three times with fresh 18.2 MΩ water and then dried at 110°C. A sample of akaganeite was also removed from an Anglo-Saxon coffin clamp. Each material was analysed by both X-ray diffractometry (Philips PW190 with Copper K_α radiation, XRD) and Fourier transform infra-red spectrometry (Perkin-Elmer 2000, FTIR) by the potassium bromide disc method to verify its identity and determine any impurities present. The materials obtained and their XRD and FTIR analyses are shown in Table 2.

Each material was roughly ground between two glass slides and was analysed with thermomagnetometry, TG and DSC. The sample size was approximately 3 mg. Thermomagnetometry was carried out on the PerkinElmer TGA7 as described previously,

Table 1 Common corrosion products of iron and their magnetic properties

Material	Magnetic structure	Magnetic susceptibility/10^{-8} m^3 kg^{-6}	Néel T_N or Curie T_C temperature/°C
iron	ferromagnetic	50,000	780 T_C
goethite α-FeOOH	antiferromagnetic	26–280	127 T_N
akaganeite β-FeOOH	antiferromagnetic	–	17 T_N
lepidocrite γ-FeOOH	antiferromagnetic	40–70	–196 T_N
limonite FeOOH·nH_2O	antiferromagnetic	66–74	
hematite α-Fe_2O_3	ferromagnetic	10–760	683 T_C
maghemite γ-Fe_2O_3	ferromagnetic	40,000–50,000	547–713 T_N
magnetite Fe_3O_4	ferromagnetic	20,000–110,000	577 T_N

Table 2 Standard materials

Material	Mineral name	Supplier	Purity	Analysis	
				XRD	FTIR
α-FeOOH	goethite	Alfa	99	goethite	
β-FeOOH	akageneite	synthesised			
β-FeOOH	akageneite	corrosion product		akageneite	
γ-FeOOH	lepidocrite	Alfa	99	lepidocrite	
Fe_3O_4	magnetite	ALD	99.5	magnetite	contains silicate
α-Fe_2O_3	hematite	ALD	99.98	hematite	
γ-Fe_2O_3	maghemite	Alfa	99.8	maghemite	
$FePO_4·2H_2O$	strengite	ALD	99.98	strengite	
FeS_2	pyrite	RT Min	–	pyrite	
$FeCO_3$	siderite	RT Min	–	siderite	
$FeCO_3$	siderite	RT Min	–	siderite	contains silicate
$FeCO_3$	siderite	RT Min	–	siderite	contains silicate
$FeSO_4·4H_2O$	rozenite	ALD		rozenite	

Alfa: Alfa Aesar, ALD: Aldrich, RT Min: Richard Taylor Minerals Ltd, –: no purity stated, mineral samples

but with a constant heating rate of 10 to 800°C. Shimadzu TGA50 and DSC50 were used with open alumina crucibles under 60 cm^3 min^{-1} of nitrogen, with a heating rate of 10 K min^{-1}. The TG was heated between 20 and 980°C, and the DSC to 650°C. The residue from each analysis was analysed with Fourier transform infra-red spectroscopy, FTIR and Raman spectroscopy, Dilor infinity with 532 nm laser excitation, for identification. When intermediate products were indicated by the thermal analyses, interrupted runs were undertaken on a PerkinElmer DSC7 and the materials analysed after heating to intermediate temperatures.

Application to accelerated corrosion tests

A series of accelerated corrosion tests was undertaken to optimise production of a model material to mimic terrestrial archaeological iron. Iron discs were pressed, as before, at masses of approximately 70 mg. The discs were buried at a depth of 10 mm in cristabolite sand XP3 (Hepworth Minerals and Chemical Limited) in glass tubes. Various solutions were added to the sand, in a mass ratio of 2.3 g of solution to 9.3 g of sand. This figure was selected to give a saturation of 60% of the maximum water holding capacity of the sand. This water content has been found to give the maximum corrosion rate in porous media [9]. The test for each solution was carried out in triplicate. The solutions are shown in Fig. 5. The tubes were sealed with polyethylene caps and heated at 70°C. The tests were dis-assembled after 28 and 56 days, the iron coupons were retrieved, the excess XP3 gently removed and the discs analysed with thermomagnetometry.

The amount of water was calculated from the mass drop between 30 and 150°C. Although this temperature is somewhat higher than normally used, the long dwell time at 150°C allowed the water loss to be viewed easily if the graph was plotted *vs*. time. It also reduced the time taken for the overall analysis, an important factor with the relatively large number of samples to be processed. The amounts of residual iron and hence the mass loss of iron, were calculated from the apparent mass drops at 780°C. Magnetite was quantified from the apparent mass drop at 580°C.

Application to archaeological ironwork

A series of nails from a 4th century AD site were analysed. The feasibility of using such material for comparative experiments was being investigated. Several samples were cut from each nail down the length of its body. A 1st century AD cart burial from East Yorkshire produced two iron tyres with diameters in excess of 1.3 m. They are extensively mineralised, with a void running through their centers, bounded by two bands of a grey, lustrous material. The tyres rapidly deteriorated after excavation and the amount of residual iron was assessed. The very large volume of the tyres and their heterogeneous state of preservation presented problems for any analytical technique. Radiography was used to guide sampling. Six areas were sampled and duplicate thermomagnetometry analyses were undertaken on each sample. The heating schedule was modified slightly with a longer dwell time at 150°C, to allow moisture to be lost from the compact corrosion and soil layers. TG was also undertaken to help clarify the magnetic nature of the transitions observed. The exhaust from the TG chamber was fed over a Vaisala carbon dioxide probe to confirm the decomposition of carbonates during the analysis.

Results

Thermomagnetometry

A typical result from thermomagnetometry for one of the iron nail samples is shown in Fig. 1. A sharp rise in apparent mass can be seen when the magnet was applied at 150°C. Despite the nitrogen purge gas, some oxidation of the iron occurs, which is observed as a steady mass increase. A drop in the mass is observed between 250 and 400°C, due to the dehydroxylation of goethite and lepidocrite. The two effects are observed as two peaks in the derivative, shown as the expanded inset in Fig. 1. A mass drop occurs at 580°C, this is due to the Néel temperature of magnetite. At 780°C the loss of ferromagnetism of the iron appears as a sharp mass loss.

The calibrations for mass produced very good linear fits and were found to be reproducible, with very similar slopes (0.0241 and 0.0244) produced from two calibrations undertaken a month apart. The graphs *vs*. mass are shown in Fig. 2. Repeatability was assessed using five discs of exactly 74 mg mass and was found

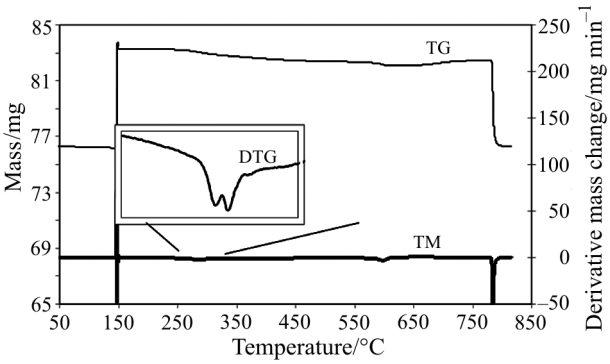

Fig. 1 Thermomagnetometry of sample from iron nail with zoom of 250–350°C region of derivative

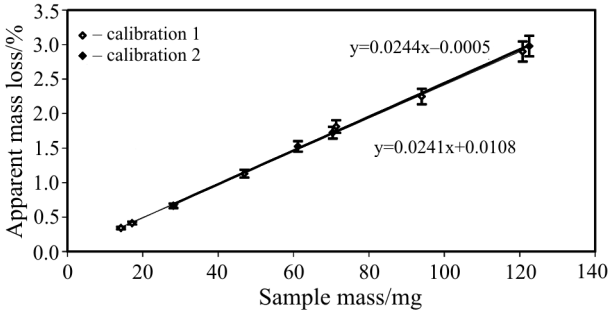

Fig. 2 Thermomagnetometry calibration *vs*. different masses of iron

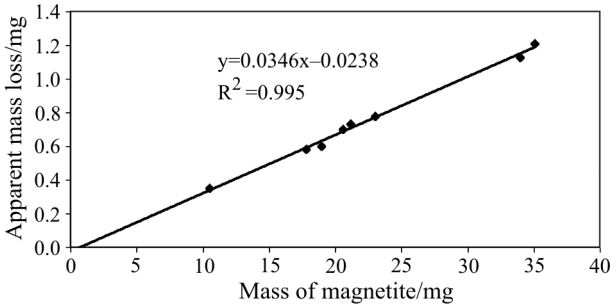

Fig. 3 Calibration for magnetite in mixed samples

to be very good, with a standard deviation in the apparent mass change of less than 0.23%. Converting these figures to mass of iron, using the calibrations developed previously, gives values between 74.07 and 74.21 mg, with a standard deviation of 0.091 mg.

The calibration graphs for the mixed discs for iron and magnetite are shown in Figs 2 and 3. The technique is slightly more sensitive to the magnetite used, with a coefficient of 0.0346 compared to 0.0240 for iron. This is consistent with the magnetic susceptibilities reported in Table 1.

The reported and measured transitions and thermal behaviour are summarised in Tables 3–5. None of the materials would interfere with the analysis of magnetite or iron. Siderite, $FeCO_3$ shows a mass loss, with the carbonate decomposing between 450 and 530°C, generating maghemite which is observed in thermomagnetometry. Siderite, akaganeite and lepidocrite all generate maghemite during thermal decomposition. Whether this occurs below the Néel temperature and would be detected by thermomagnetometry depends on the crystallite size and degree of crystallinity of the precursors. These reactions could possibly interfere with the analysis of other maghemite present. However this mineral has only very rarely been reported on archaeological iron. Both akaganeite and lepidocrite should be distinguishable from their lower temperature dehydroxylation reactions.

Application to accelerated corrosion tests

The results from the series of accelerated corrosion tests are shown in Fig. 4. After 28 days the less concentrated chloride solutions had only magnetite detected as the corrosion. Iron loss was not detected because of the iron's greater measurement uncertainty. The magnetite obviously originated from the loss of iron, but this is below the detection limit of the method. At higher chloride concentrations and longer reaction times, iron loss was readily determined. As one would expect, both increasing the chloride concentration and decreasing the initial pH (using HCl instead of NaCl) increased the rate loss of iron. The water content of the corrosion products increased with the degree of reaction as porous corrosion products were formed. The corrosion products also adhered the cristabolite sand to the iron, again generating porosity, which held water.

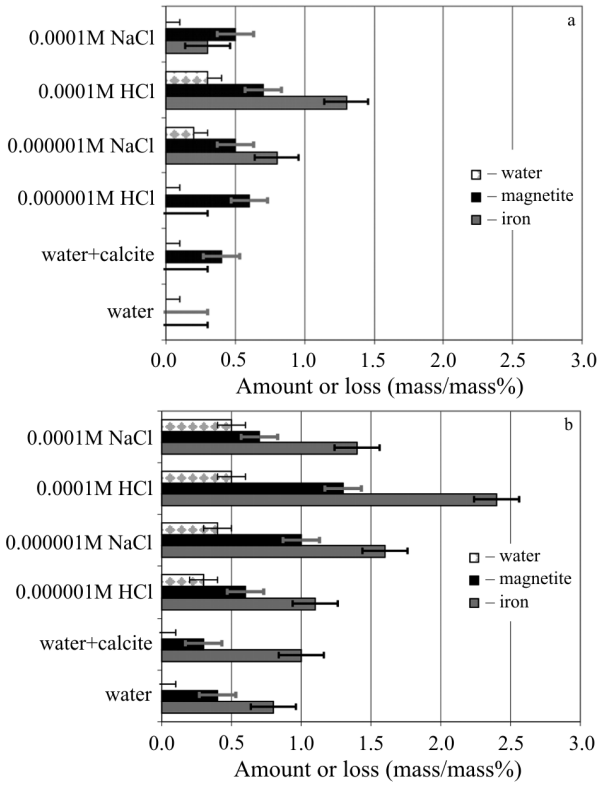

Fig. 4 Accelerated corrosion: upper 28 days, lower 56 days

Application to archaeological ironwork

A set of analyses from one nail is shown in Fig. 5. As can be seen the degree of corrosion and relative amounts of corrosion products varies dramatically down the length of the nail. It would be extremely difficult to use such a sample for comparative experiments. Representative analyses from the tyres are shown in Fig. 6. A

Table 3 Literature values of thermal transitions

T_{range} of transition/°C	Mass loss/%	Reactant	Product	Reference	Technique
		goethite α-FeOOH			
190–380*	10.10	goethite	hematite	10	DTA
258–320	10.34–11.29	goethite		11	DTA, TG
		akaganeite β-FeOOH			
270–320		akaganeite	maghemite	12	TG, XRD, ED, HREM
340–367	–	maghemite	hematite		
(250–300)		(akaganeite)	(maghemite)	(13)	(DTA)
(400–450)	(–)	(maghemite)	(hematite)		
125–300		akaganeite	maghemite	10	DTA
	–	maghemite			
		lepidocrite γ-FeOOH			
220–270		lepidocrite	maghemite	14	
435–510	–	maghemite	hematite		
(270)		(lepidocrite)	(maghemite)	(15)	
(500)	(–)	(maghemite)	(hematite)	(16)	
300–350	10.10	lepidocrite	maghemite	10	DTA
400–500	–	maghemite	hematite		
		feroxyhyte δ-FeOOH			
150–230		feroxyhyte	NS	8	DTA
(100–320)		(feroxyhyte)	(hematite)	(10)	(DTA)
		ferrihydrate $Fe_5HO_8·4H_2O$			
150–230		ferrihydrate	NS	17	DTA
280–320		NS	hematite		
		magnetite Fe_3O_4			
350–400		magnetite	maghemite	10	DTA
650–800		maghemite	hematite	10	
		maghemite γ-Fe_2O_3			
397–597*		maghemite	hematite	18	XRD, dilatometry, TM
(275–800)		(maghemite)	(hematite)	(19)	
		siderite			
400–550		siderite	magnetite*	20	TG, TM, EGA, XRD
		pyrites			
440–667		pyrites	pyrrhotite	21	TG, XRD

NS: not specified, XRD: X-ray diffraction, ED: electron diffraction, HREM: high resolution electron microscopy, EGA: evolved gas analysis, Hematite has no reported thermal transitions below 1000°C

large amount of magnetite was indicated by the large apparent mass loss at 580°C. This effect was not observed with TG. Aside from water, two other mass losses were observed, one occurring between 400 and 500°C, and the other 650 and 700°C on both TM and TG. These were tentatively assigned to iron carbonate, siderite and calcium carbonate, calcite, respectively. Large amounts of carbon dioxide were evolved by two thermal events. The identifications were verified with FTIR spectroscopy. Absorption bands characteristic of both the calcium carbonate (1798, 1422, 874, 712 cm^{-1}) and iron carbonate (1414, 866 and 712 cm^{-1}) were observed, confirming the presence of these materials. Magnetite was confirmed by the presence of peaks at 308, 542 and 667 cm^{-1} with Raman spectroscopy. Elemental iron was detected with thermomagnetometry, in only one of the six samples and occurred as a very thin sheet in the centre of the void. The radiographs showed this was localised to one very small (less than 1 cm) portion of the tyres.

Table 4 TG and TM results

	Measured onset T/°C	Measured endset T/°C	Mass loss/%	
goethite α-FeOOH	267	309	9.111	dehydroxylation
akaganeite β-FeOOH synthetic	253	451	9.820	dehydroxylation
akaganeite β-FeOOH corrosion	236	443	10.379	dehydroxylation
lepidocrite γ-FeOOH	210	265	11.107	dehydroxylation
	(374)	(425)	(–1.180)	
	(425)	(480)	(2.498)	Néel temperature
(magnetite Fe_3O_4)	(558)	(667)	(22.325)	Néel temperature
(hematite α-Fe_2O_3)	(683)	(713)	(0.161)	Néel temperature
maghemite γ-Fe_2O_3	steady increase from 328°C		~4%	oxidation
	(333)	(685)	(29.483)	Néel temperature
strengite $FePO_4{\cdot}2H_2O$	133	177	13.035	dehydration
	(506)	(583)	(2.534)	
pyrites FeS	461	515	3.056	
	957	974	1.799	
	(554)	(559)	(2.488)	Néel tempreature
	(595)	(722)	(12.694)	Néel temperature
rozenite $FeSO_4{\cdot}4H_2O$	106	138	27.035	dehydration
	461	515	3.056	
	957	974	1.799	
siderite $FeCO_3$	458	507	29.597	

Thermomagnetometric effects are in brackets

Table 5 DSC results

Compound	Peak	Onset	Endset	Enthalpy/ J g^{-1}	Product		
					FTIR peaks/cm^{-1}	Raman peaks/cm^{-1}	identification
goethite	298	283	311	–196.6	645, 525, 440	226, 292, 411, 612	hematite
akaganeite	207	175	254	–137.0	461, 580, 642, 704, 3675	381, 486, 670	maghemite
syn	592	571	606	72.0	646, 525, 440	226, 292, 411, 497, 612	hematite
akaganeite	303	278	340	–228.7	459, 580, 646, 700, 3677	381, 670	maghemite
corrosion	568	538	637	102.9	643, 526, 441	226, 292, 411, 612	hematite
lepidocrite	57	32	82	–34.5	750, 1018	252, 379, 638	lepidocrite
	250	219	270	–143.0	459, 580, 650, 701, 3675	381, 486, 670, 718	maghemite
	446	432	462	55.8	645, 525	226, 292, 245, 411, 612	hematite
magnetite	396	311	448	62.6	647, 525, 440	226, 292, 411, 497, 612	hematite
hematite	no transitions observed						
maghemite	584	556	614	–26.8	645, 526, 441	226, 292, 612	hematite
strengite	74	33	91	–24.2	589, 1039, 1634, 3372	not done	iron phosphate hydrate
	145	129	162	–78.0	589, 1039	not done	
	580	527	592	21.9	645, 525, 440	226, 292, 411, 612	iron phosphate hematite
pyrites	149	145	156	–7.2	none	none	
	554	457	480	–12.3	645, 525, 440	226, 292, 411, 497, 612	hematite
siderite	411	406	433	–293.2	460, 580, 650, 700, 3675	381, 486, 670, 718	maghemite
	536	521	561	–11.5	645, 525	226, 292, 245, 411, 612	hematite
rozenite		583	707	29.589	645, 525, 440	226, 292, 411, 612	hematite

Negative values are endothermic

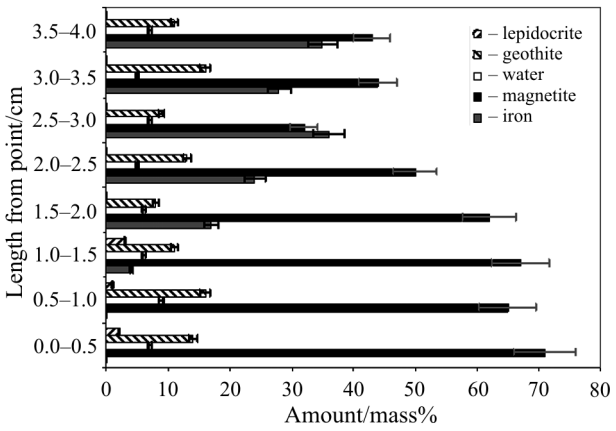

Fig. 5 Analysis of nail samples

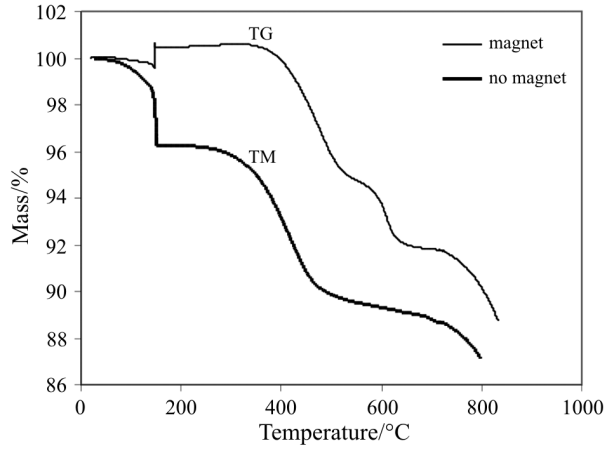

Fig. 6 TG and thermomagnetometry of archaeological tyre samples

It would appear that the tyres were at the very end of the mineralisation process when excavated. Despite this they underwent rapid physical deterioration, with akaganeite forming in the central void and splitting them apart. The burial was discovered with a metal detector and it appears that the magnetic component detected was the magnetite.

Conclusions

Thermomagnetometry has provided a viable alternative or valuable complement to stripping treatments for determining the content of elemental iron. It also provides a rapid quantification of the magnetite and water content. An analysis can be completed under 20 min. The technique has the potential to allow further quantification of other corrosion products such as goethite or lepidocrite, but this requires a lower heating rate and longer analysis times. It has also found utility to determine the presence of any residual iron in archaeological iron artefacts.

References

1 ASTM G1 - 90, Standard practice for preparing, cleaning and evaluating corrosion test specimens. American Society for the Testing of Materials, Conshohocken, PA, USA 1999.
2 D. Watkinson, Studies in Conservation, 28 (1983) 85.
3 IUPAC, Compendium of Chemical Terminology, 1997, p. 1740.
4 S. S. J. Warne, H. J. J. Hurst and W. I. Stuart, Therm. Anal. Abs., 17 (1998) 1.
5 P. K. Gallagher, J. Thermal Anal., 49 (1997) 33.
6 B. Knight, The Conservator, 14 (1990) 37.
7 U. Bleil and N. Petersen, Physical Properties of Rocks, edited by G. Angenheister, Springer-Verlag, New York 1982, pp. 308–432.
8 R. M. Cornell and U. Schwertmann, The Iron Oxides, VCH BverlagsgesellschaftmbH, Weinheim 1986, p. 490.
9 C. P. Gardiner and R. E. Melchers, Corr. Sci., 44 (2002) 2459.
10 R. C. MacKenzie, Differential Thermal Analysis, Academic Press, London 1970.
11 U. Schwertmann, P. Cambier and E. Murad, Clays Clay Min., 33 (1985) 369.
12 J. M. Gonzalez-Calbet and M. A. Alario Franco, Thermochim. Acta, 58 (1982) 45.
13 E. Paterson, R. Swaffield and D. R. Clark, Thermochim. Acta, 54 (1982) 201.
14 A. R. Dinesen, C. T. Pedersen and C. Bender Koch, J. Therm. Anal. Cal., 62 (2001) 1303.
15 U. Schwertmann and E. Wolska, Clays Clay Min., 38 (1990) 209.
16 E. Wolska, W. Szajda and P. Piszora, J. Thermal Anal., 38 (1992) 2115.
17 L. Carlson and U. Schwertmann, Geochim. Cosmochim. Acta, 45 (1981) 421.
18 E. Karmazsin, P. Satre and P. Vergnon, J. Thermal Anal., 28 (1983) 279.
19 R. M. Bozorth, Ferromagnetism, van Nostrand, New York 1951, p. 242.
20 P. K. Gallagher and S. S. J. Warne, Thermochim. Acta, 43 (1981) 253.
21 H. Hu, Q. Chen, Z. Yin and P. Zhang, Thermochim. Acta, 398 (2003) 233.